Proceedings of the
44th IEEE Conference on Decision and Control, and
the European Control Conference 2005
Seville, Spain, December 12-15, 2005

Beyond the Existence of Diagonal Controllers: from the Relative Gain Array to the Multivariable Structure Function

Eduardo Licéaga-Castro, *Member, IEEE*, Jesús Licéaga-Castro, and Carlos E. Ugalde-Loo, *Member, IEEE*

***Abstract*—A study related to coupling measurement and the existence of diagonal controllers for multivariable linear systems is presented. It is shown that the relative gain array (RGA) can be expressed in terms of the multivariable structure function (MSF). Moreover, the appropriate interpretation and handling of the MSF allows: (a) to establish the dynamical structure of the multivariable control system, (b) to prove the existence of stabilising diagonal controllers, (c) to determine whether design specifications can be met, and (d) the general coupling measurement among channels. In order to show the application of the MSF to the analysis and design of diagonal controllers, a family of plants is studied, ranging from non coupled minimum–phase to highly coupled and non–minimum phase plants. The actual multivariable control designs are included for completeness. The examples here presented may be a good benchmark for further analysis and comparisons.**

I. Introduction

Given a multivariable control design problem, it is convenient to establish if design specifications can be met by means of diagonal controllers since they are easier to analyse and implement. This approach is called decentralised control [2,8,9]. A technique based on the relative gain array (RGA) matrix is used to determine if it is possible to design decentralised control systems. This topic is studied in [2,9]. Under a different approach based on classical techniques, the multivariable structure function (MSF) for analysing control structures with diagonal controllers was introduced in [3,4].

In this paper the analysis and design of diagonal controllers using the RGA and MSF are presented. Along this work it is shown that an appropriate interpretation of the MSF gives an effective and complete framework (*not a method*) for analysing and designing multivariable control systems. For instance, the MSF proved very helpful in proposing a new solution to the control problem of an induction motor [11,12]. It is also shown that the RGA can be expressed in terms of the MSF –both contain the same information. Nevertheless, it is demonstrated that by an appropriate interpretation of the MSF at low and high frequency it is possible to determine: the existence and the required dynamical structure of diagonal controllers, the dynamical structure of the closed–loop system, a reliable measurement of robustness, and the possibility to satisfy design specifications. The analysed plants are the elements of a family of plants suggested in [2]. It should be remarked that the systems proposed there present very interesting and challenging control design problems. By adjusting two parameters of a *2x2* plant, the analysed cases vary from a decoupled to a highly coupled non–minimum phase system.

This paper is organised as follows: In Section II it is shown that the matrix related to the RGA can be expressed in terms of the MSF. In Section III, a series of cases studied in [2] through the RGA approach are analysed using the MSF. Finally, in Section IV the conclusions end the paper.

E. Licéaga-Castro is with SEPI-ESIME Ticomán IPN, Ticomán 600, Col. S.J. Ticomán, C.P. 07340, D.F., México (e-mail: eliceagac@uk2.net).

J. Licéaga-Castro is with the Mechanic and Mechatronics Engineering Department, ITESM-CEM, Carretera Lago de Guadalupe Km.3.5, Atizapán de Zaragoza,C.P.52926,Edo.México,México (e-mail: jliceaga@itesm.mx).

C.E. Ugalde-Loo is with the Department of Electronics and Electrical Eng., Faculty of Engineering, University of Glasgow, G12-8QQ, Glasgow, Scotland, UK (e-mail: kaghlus@hotmail.com).

II. Relationship Between RGA & MSF

The RGA matrix was first proposed by Bristol in [1]. His results were limited to zero frequency. Nevertheless, it is claimed in [9] that this method is effective for the whole frequency domain. The present work confirms this fact. The RGA matrix is defined as

$$\Lambda(\mathbf{G}(s)) = \mathbf{G}(s) \times \left[\mathbf{G}(s)^{-1}\right]^T \tag{1}$$

where $\mathbf{G}(s) = |g_{ij}(s)|$ is the transfer matrix of the system and X denotes the Hadamard or Schur product –the element to element product of matrices. In the case of a *2x2* matrix:

$$\Lambda(\mathbf{G}(s)) = \begin{bmatrix} \dfrac{1}{1-\gamma(s)} & \dfrac{\gamma(s)}{\gamma(s)-1} \\ \dfrac{\gamma(s)}{\gamma(s)-1} & \dfrac{1}{1-\gamma(s)} \end{bmatrix} \tag{2}$$

where

$$\gamma(s) = \frac{g_{12}(s)\, g_{21}(s)}{g_{11}(s)\, g_{22}(s)} \tag{3}$$

is defined as the multivariable structure function (MSF) [4].

The $\lambda_{ij}(s)$ elements of the $\Lambda(\mathbf{G}(s))$ matrix are interpreted as a coupling measure of the channel sensitivity from the input–*i* towards the output–*j*. Then, a system with diagonal dominance is one whose RGA matrix diagonal elements are *small*. This coupling quantification is considered empirical in [2]. Nevertheless, the interpretation of the MSF $\gamma(s)$ goes far beyond the empirical result. In [9] the properties of RGA have been treated in detail. The most important are:

1) Plants with large RGA–elements ($\gamma(s) \rightarrow 1$) should not be decoupled by inverse base controllers or decouplers.
2) Large RGA elements imply high sensitivity to (element–by–element) $\mathbf{G}(s)$ uncertainty.
3) If the sign of an RGA element changes as *s* varies from $0j$ to ∞j, there is a RHPZ in $\mathbf{G}(s)$ or in some subsystem of it.
4) For stable plants avoid input–output paring on negative steady state RGA–elements. Otherwise, if the sub-

0-7803-9568-9/05/$20.00 ©2005 IEEE

controllers are designed independently each with integral action, then the interactions will cause instability either when all the loops are closed, or when the loop corresponding to the negative relative gain becomes inactive.

These properties are better addressed using the MSF by means of the structural analysis of the individual channels. In particular, by analysing the MSF it will be clear that *the stabilisation of the diagonal elements of* ***G****(s) is not required as the structural properties* (number of RHPZs and LHPZs) *are preserved in each channel* [12]. As a consequence of this structural condition, if a controller becomes inactive instability arises –that is, lack of integrity. Analysing these properties and facts allows the use of the traditional gain and phase margins as robustness indicators for MIMO systems. It will be shown next that the RGA properties can be better explained in a clear and transparent way by the MSF.

Consider a system represented by $\mathbf{G}(s) = |g_{ij}(s)|$, $i,j=1,2$, and a diagonal controller $\mathbf{K}(s)=|K_{ij}(s)|$. The resulting input-output channels are given by (Fig. 1):

$$C_i(s) = K_{ii}(s)\, g_{ii}(s)(1-\gamma(s)\, h_j(s)) \tag{4}$$

where

$$h_i(s) = \frac{K_{ii}(s)\, g_{ii}(s)}{1+K_{ii}(s)\, g_{ii}(s)} \tag{5}$$

Notice that the MSF $-\gamma(s)-$ is of great importance since [12]

- It determines the dynamical characteristics of each input–output configuration;
- It has an interpretation in the frequency domain;
- Its magnitude quantifies the coupling between channels;
- It is related to the plant transmission zeros (zeros of $1-\gamma_a(s)$, $|\mathbf{G}(s)| = g_{11}(s)g_{22}(s) - g_{12}(s)g_{21}(s) = 0$);
- $\gamma_a(s)=1$ determines the non–minimum phase condition;
- Its closeness to $(1,0)$ in the Nyquist plot indicates to what extent the plant is sensitive to uncertainty in terms of gain and phase margins.

It can be proved that the closed loop system is given by [12]:

$$y_i(s) = R_i(s) r_i(s) + P_i(s) Q_i(s) r_j(s) \tag{6}$$

$$R_i(s) = \frac{C_i(s)}{1+C_i(s)}, P_i(s) = \frac{1}{1+C_i(s)}, Q_i(s) = \frac{g_{ij}(s)\, h_j(s)}{g_{jj}(s)} \tag{7,8,9}$$

In [12] it is shown that in order to stabilise the closed loop response (6) it is just necessary to stabilise the channels $C_i(s)$. In other words, if $K_{ii}(s)$ stabilises the channels (4), it will also stabilise the closed loop response (6).

The closed loop system dynamical structure with a diagonal controller is summarised in Table I.

Notice that the coupling can be expressed in *dB* directly from the channels (4) by means of functions $\gamma(s)h_j(s)$. While using matrix (2) the coupling measure is reduced to a range between $0–1$, through the MSF it is possible to determine the dynamical structure of the system using Table I and analysing the Nyquist plot of $(1-\gamma(s)h_j(s))$. Note that the system is ill–conditioned (minimum phase) as $\gamma(s)\rightarrow 1$ ($\Lambda(\mathbf{G}(s))\rightarrow[\infty]$). If $\gamma(s)=1$, $\mathbf{G}(s)$ is non–minimum phase.

The controller design based on the MSF is named *Individual Channel Design* (ICD) and it was first introduced in [3,4]. An analysis in terms of Table I and the MSF $\gamma(s)$ for a series of cases studied in [2] using RGA is reviewed below within the MSF framework.

III. Analysis and Design of Typical Cases

In reference [2] a family of *2x2* multivariable plants is considered, $\mathbf{Y}(s) = \mathbf{G}(s)\mathbf{u}(s)$, where the elements of $\mathbf{G}(s)$ are:

$$g_{11}(s) = \frac{2}{s^2+3s+2}, g_{12}(s) = \frac{k_{12}}{s+1}$$
$$g_{21}(s) = \frac{k_{21}}{s^2+2s+1}, g_{22}(s) = \frac{6}{s^2+5s+6} \tag{10}$$

The RGA matrix for (10) is given by

$$\Lambda(\mathbf{G}(s)) = \begin{bmatrix} \frac{1}{1-k_{12}k_{21}} & \frac{-k_{12}k_{21}}{1-k_{12}k_{21}} \\ \frac{-k_{12}k_{21}}{1-k_{12}k_{21}} & \frac{1}{1-k_{12}k_{21}} \end{bmatrix} \tag{11}$$

In [2], the analysis of the family of plants defined by (10) according to RGA is presented. The elements of this family correspond to different values of k_{12} and k_{21}. Each set of values present a different control design challenge, ranging from a simple decoupled case to a highly coupled non–minimum phase plant. It should be remarked that for difficult situations the RGA cannot give a conclusive answer about the best way to design a diagonal controller. As follows it is shown that the MSF can give full information about the system structure and design of the controller itself.

The following design specifications are considered: gain and phase margins of at least *20 dB* and *60°* respectively; a maximum overshoot of *10%* and a settling time less than *3s*.

Note. The MSF obtained from pairing y_1-u_1 and y_2-u_2 is:

$$\gamma_a(s) = \frac{g_{12}(s)\, g_{21}(s)}{g_{11}(s)\, g_{22}(s)} \tag{12}$$

If the channels are defined by pairing y_1-u_2 and y_2-u_1, then

$$\gamma_b(s) = \frac{g_{11}(s)\, g_{22}(s)}{g_{12}(s)\, g_{21}(s)} \tag{13}$$

is the resulting MSF. The following designs were obtained with the aid of the Toolbox reported in [10].

A. Case 1 ($k_{12} = k_{21} = 0$)

It is clear that the case is trivial since it reduces to two independent SISO plants. Then $\gamma_a(s) = 0$ and $\gamma_b(s) = \infty$ for any frequency. For instance, the RGA matrix is

$$\Lambda = \begin{bmatrix} 1 & 0 \\ 0 & 1 \end{bmatrix} \tag{14}$$

which provides the same information given by the MSFs. In [2] a design is proposed considering diagonal elements.

B. Case 2 ($k_{12} = k_{21} = 0.1$)

In [2] a SISO design with the pairing corresponding to $\gamma_a(s)$ keeping the controller of *Case 1* is suggested, since

$$\Lambda = \frac{100}{99}\begin{bmatrix} 1 & -0.01 \\ -0.01 & 1 \end{bmatrix} \tag{15}$$

and point 4 of Section II. The following analysis shows that the alternative input–output channel definition is also

possible. The system in this case is non–minimum phase, but the culprit zero is at a very high frequency, thus the non–minimum phase zero does not hamper the design.

1) Analysis with $\gamma_a(s)$: The related MSF is

$$\gamma_a(s) = 0.0008333 \cdot \frac{(s+3)(s+2)^2}{(s+1)^2} \tag{16}$$

The input–output channels are:

$$C_i(s) = K_{ii}(s)\, g_{ii}(s)\left(1 - \gamma_a(s)\, h_j(s)\right) \tag{17}$$

The existence and design of the controllers $K_{11}(s)$ and $K_{22}(s)$ are determined by the characteristics of $\gamma_a(s)$, which are revealed by their Nyquist and Bode diagrams shown in Fig. 2. Those characteristics are analysed as follows.

(a.1) The magnitude of $\gamma_a(s)$ at low frequencies is small: *–40 dB*. Moreover, $1 - \lim_{s\to\infty} \gamma_a(0) > 0$. Nevertheless, at *3 rad/s* it increases at a rate of *20 dB/dec*. While $s \to \infty$, $|\gamma_a(s)| \to \infty$, so $1 - \lim_{s\to\infty} \gamma_a(s) < 0$. However, the Nyquist path of $\gamma_a(s)$ is not to the left of *(1,0)* at high frequencies. As matter of fact, it is easy to check that $\gamma_a(s)$ encircles clockwise *(1,0)* once.

(a.2) Function $\gamma_a(s)$ has no RHPPs and its Nyquist diagram encircles clockwise *(1,0)* once. Then, according to Table I and the Nyquist stability criterion, $(1-\gamma_a(s))$ has one RHPZ. However, such a zero is at a very high frequency.

(a.3) Due to **(a.1)** and **(a.2)**, functions $h_i(s)$ influence the channel structure at high frequencies. In fact, it may be required to limit their bandwidth in order to avoid the encirclements of *(1,0)* by $(1-\gamma_a(s)h_i(s))$. Obviously, this characteristic will be reflected by the design on $h_i(s)$. Notice that at low frequencies $|\gamma_a(s)| < 1$. In general, it is desired not only that $\gamma_a(s)$ and $\gamma_a(s)h_i(s)$ preserve the same number of encirclements to *(1,0)*, but also that their Nyquist plots do not pass near *(1,0)*. Otherwise the system will be very sensitive to uncertainty. The structure of the system can be preserved if the cut–off frequency of each channel is induced at those frequencies where the Nyquist plot of $\gamma_a(s)h_i(s)$ lies to the left from *(1,0)*. In other words, it is just necessary to achieve an adequate roll–off of $h_i(s)$ in order to preserve adequate robust and performance specifications.

(a.4) The transfer functions $g_{ii}(s)$ are minimum phase and stable. Then, provided that $h_i(s)$ are stable, in

$$\gamma_a(s)\, h_i(s) = \frac{g_{ij}(s)\, g_{ji}(s)}{g_{ii}(s)\, g_{jj}(s)} \cdot \frac{K_{ii}(s)\, g_{ii}(s)}{1 + K_{ii}(s)\, g_{ii}(s)}$$

no cancellations of RHPPs from $\gamma_a(s)$ with RHPZs from $h_i(s)$ occur. The structure of $(1-\gamma_a(s))$ is preserved by $(1-\gamma_a(s)h_i(s))$ if $K_{ii}(s)$ stabilises $g_{ii}(s)$ and the channel. The encirclement of *(1,0)* at high frequencies is avoided by inducing a cut–off frequency with an adequate roll–off slope of $\gamma_a(s)h_i(s)$.

The existence of the channel controllers is reduced to those $K_{ii}(s)$ which stabilise simultaneously $g_{ii}(s)(1-\gamma_a(s)h_j(s))$ and $g_{ii}(s)$ ($i,j = 1,2,\ i \neq j$). According to the above analysis it is possible to design stabilising controllers. For instance:

$$K_{11}(s) = \frac{3.6(s+1.07)(s+1)}{s(s+1.95)}, K_{22}(s) = \frac{140(s+1.5)}{s(s+100)}$$

The structural robustness of the channels and the control system are shown in Table II in the format introduced in [12]. The information associated to Table II, as well the controller performance, is shown in Fig. 3.

It should be mentioned that the coupling at high frequencies has been substantially reduced as indicated by the plots of $\gamma_a(s)h_i(s)$ (Fig. 3).

2) Analysis with $\gamma_b(s)$: The related MSF is

$$\gamma_b(s) = 1200 \cdot \frac{(s+1)^2}{(s+3)(s+2)^2} \tag{18}$$

and the channels and functions $h_i(s)$ are defined by:

$$C_i(s) = K_{ij}(s)\, g_{ji}(s)\left(1 - \gamma_b(s)\, h_j(s)\right), \quad h_j(s) = \frac{K_{ji}(s)\, g_{ij}(s)}{1 + K_{ji}(s)\, g_{ij}(s)} \tag{19}$$

The Nyquist and Bode diagrams of $\gamma_b(s)$ are shown in Fig. 4 and its characteristics are analysed as follows:

(b.1) It is noted that $1-\gamma_b(0)<0$ and has a very large value: *40 dB*. This means that the Nyquist plot of $\gamma_b(s)$ starts to the right of *(1,0)*. On the other hand, when $s \to \infty$, $1 - \lim_{s\to\infty} \gamma_b(s) > 0$, thus $\gamma_b(s)$ ends on the left from *(1,0)*.

(b.2) Function $\gamma_b(s)$ has no RHPPs and its Nyquist diagram encircles clockwise *(1,0)* once. Then, $(1-\gamma_b(s))$ has one RHPZ. From the Bode plot of $\gamma_b(s)$ it is possible to observe that the RHPZ is located at a frequency above *1000 rad/s*.

(b.3) From **(b.1)** and **(b.2)** it is possible to conclude that the signs of the numerators of the channels change at the RHPZ frequency. Thus, the bandwidth of the channels should be less than the RHPZ.

(b.4) Assuming that $h_2(s)$ is stable $(h_2(0>0)$, the structure of $(1-\gamma_b(s))$ is preserved by $(1-\gamma_b(s)h_2(s))$. Thus, channel C_1 can be stabilised with a controller $K_{12}(s)$, such that $K_{12}(0) < 0$, provided that $h_2(s)$ induces a roll–off before the RHPZ.

(b.5) The controller described in **(b.4)** stabilises Channel 1 and induces one RHPP on $h_1(s)$ ($K_{12}(0)<0,\ h_1(0)>0$), provided that the controller contains an integrator and $h_1(0)>0$. Note that $h_1(s)$ changes its sign at high frequency.

(b.6) From **(b.4)** and **(b.5)** the function $\gamma_b(s)h_1(s)$ encircles counter clockwise *(1,0)* once. Thus, by applying the Nyquist criterion $(1-\gamma_b(s)h_1(s))$ has no RHPZs. Therefore, Channel 2 is minimum phase.

(b.7) In order to stabilise the multivariable system, $K_{12}(s)$ should stabilise (21) and induce one RHPP in $h_1(s)$, and $K_{21}(s)$ should stabilise (22) and $h_2(s)$.

REMARK. The stabilisation with diagonal controllers does not generally imply stabilisation of the diagonal elements.

For instance, the following controllers were obtained:

$$K_{12}(s) = \frac{-0.75(s+2)(s+1)}{s(s+10)}, K_{21}(s) = \frac{37.9(s+1)(s+0.1)}{s(s+3.03)}$$

The structural robustness of the channels and the control system are shown in Table III. The information associated to Table III and the controller performance are shown in Fig. 5.

C. Case 3 ($k_{12} = –1$, $k_{21} = 0.5$)

For this case, the RGA matrix is given by

$$\Lambda = \frac{1}{3}\begin{bmatrix} 2 & 1 \\ 1 & 2 \end{bmatrix} \tag{20}$$

which suggests a design with the pairing corresponding to $\gamma_a(s)$. In this situation coupling starts to show. Nevertheless, the designs considering both input–output pairing do not present any particular problem according to the MSF. The system is stable and minimum phase.

1) Analysis with $\gamma_a(s)$: The related MSF is

$$\gamma_a(s) = -0.041667 \cdot \frac{(s+3)(s+2)^2}{(s+1)^2} \tag{21}$$

and the channels are defined by (17). The characteristics of $\gamma_a(s)$ are shown in Fig. 6 and discussed next.

(a.1) The magnitude of $\gamma_a(0)<1$ and the Nyquist diagram of $\gamma_a(s)$ is located to the left of $(1,0)$ for any s.

(a.2) Function $\gamma_a(s)$ has no RHPPs and its Nyquist diagram does not encircle $(1,0)$ at all. Thus, $(1-\gamma_a(s))$ has no RHPZs.

(a.3) Due to **(a.1)** and **(a.2)**, $h_i(s)$ do not influence the channel structure provided that they are stable. Nevertheless, the coupling increases with frequency at a rate of *20 dB/dec* (Fig. 6). In order to counteract this effect it is necessary to have $h_i(s)$ with a roll–off slope of at least *–40 dB/dec*.

(a.4) $g_{ii}(s)$ are minimum phase and stable. No cancellations involving RHPPs of $\gamma_a(s)$ with RHPZs of $h_i(s)$ occur. Thus, the structure of $(1–\gamma_a(s))$ is preserved by $(1–\gamma_a(s)h_i(s))$.

The controller existence is reduced to $K_{ii}(s)$ which stabilise $g_{ii}(s)(1–\gamma_a(s)h_j(s))$ and $g_{ii}(s)$ simultaneously. For instance:

$$K_{11}(s) = \frac{3.5(s+1)(s+0.7)}{s(s+1.95)}, K_{22}(s) = \frac{1400(s+1)}{s(s+1000)}$$

The structural robustness of the channels is summarised in Table IV and Fig. 7.

2) Analysis with $\gamma_b(s)$: The associated MSF is

$$\gamma_b(s) = -24 \cdot \frac{(s+1)^2}{(s+3)(s+2)^2} \tag{22}$$

and the channels are defined as in (19). The Nyquist and Bode plots related to this case are shown in Fig. 8. Such characteristics are analysed below.

(b.1) The magnitude of $\gamma_b(s)$ while $s \to \infty$ is less than one (in fact zero), so $1 - \lim_{s\to\infty} \gamma_b(s) > 0$; in addition $\gamma_b(0)=–2$. In fact, the Nyquist plot of $\gamma_b(s)$ is always to the left of $(1,0)$ for all s.

(b.2) Function $\gamma_b(s)$ has no RHPPs and its Nyquist plot does not encircle $(1,0)$. Thus, $(1-\gamma_b(s))$ does not contain RHPZs.

(b.3) Due to **(b.1)** and **(b.2)**, stable and minimum phase $h_i(s)$ do not influence the channel structure at high frequencies. The numbers of encirclements to $(1,0)$ by $\gamma_b(s)$ and $\gamma_b(s)h_i(s)$ coincide. Nevertheless, the coupling between the channels is relatively high at *2 rad/s* (Fig. 8). It can be reduced if $h_j(s)$ has an appropriate roll–off slope.

(b.4) Since $g_{ij}(s)$ $(i,j=1,2,i\neq j)$ are minimum phase, products $\gamma_b(s)h_j(s)$ have no cancellations. Thus, the structure of $(1–\gamma_b(s))$ is preserved by $(1–\gamma_b(s)h_j(s))$ provided $h_j(s)$ are stable.

The existence of controllers is reduced to $K_{ij}(s)$ which simultaneously stabilise $g_{ji}(s)$ and the channel. For example:

$$K_{12}(s) = \frac{25(s+1)^3}{s(s+5)^2}, K_{21}(s) = \frac{-1.24(s+3)(s+2)^2}{s(s+4)^2}$$

The structural robustness of the channels and control system are shown in Table V. The information associated to it and the controller performance are shown in Fig. 9.

D. Case 4 ($k_{12} = –2$, $k_{21} = –1$)

This is a rather interesting and challenging case. The system is non–minimum phase and in the pairing corresponding to $\gamma_a(s)$ the coupling is high. This is certainly one of those surprising issues that can arise when MIMO interactions are ignored [2]. The controller proposed in [2] results in an unstable closed loop system. For instance, the RGA matrix is

$$\Lambda = \begin{bmatrix} -1 & 2 \\ 2 & -1 \end{bmatrix} \tag{23}$$

which suggests a design with the pairing corresponding to $\gamma_b(s)$ since the diagonal entry is negative. Nevertheless, diagonal stabilising controllers for both pairings exist. Of course the performance will be limited, but these limits can be clearly established from the analysis of the MSF.

1) Analysis with $\gamma_a(s)$: The corresponding MSF is

$$\gamma_a(s) = 0.16667 \cdot \frac{(s+3)(s+2)^2}{(s+1)^2} \tag{24}$$

and the input–output channels are defined by (17). The corresponding Nyquist and Bode plots are shown in Fig. 10. Such characteristics are analysed as follows:

(a.1) The value of $\gamma_a(0)>1$ (in fact, $\gamma_a(0)=2$) and the Nyquist diagram of $\gamma_a(s)$ starts at the right side of $(1,0)$. Also, $\gamma_a(s)$ has no RHPPs and its Nyquist path encircles clockwise $(1,0)$ twice. Therefore, $(1–\gamma_a(s))$ contains two RHPZs.

(a.2) If $h_2(0)>0.5$ and stable then $(1–\gamma_a(0)h_2(0))<0$. Thus, a stabilising controller $K_{11}(s)$ is such that $K_{11}(0)<0$. On the other hand, $g_{11}(0)>0$; therefore, $h_1(s)$ is unstable with one RHPP. Also, if $|K_{11}(0)g_{11}(0)| > 0$, then $h_1(0)>0$.

(a.3) If **(a.1)** and **(a.2)** hold, then $g_{22}(0)(1–\gamma_a(0)h_1(0))>0$; thus, a stabilising controller $K_{22}(s)$ is such that $K_{22}(0)>0$. Moreover, if the relative degree of $h_1(s)$ is greater than the relative degree of $\gamma_a(s)$, then $\gamma_a(s)h_1(s)$ encircles counter clockwise $(1,0)$ once. Recall that $\gamma_a(s)h_1(s)$ has one RHPP; thus, Channel 2 is minimum–phase.

(a.4) From **(a.3),** the controller of Channel 2 should stabilise $g_{22}(s)(1–\gamma_a(s)h_1(s))$ and $g_{22}(s)$ simultaneously.

REMARK. No stabilisation of diagonal elements is required; in fact one of the diagonal elements has to be closed-loop unstable to stabilise the whole system.

Considering the previous analysis, it can be concluded that the control for this configuration exists, but it presents performance limitations (Channel 1 has 2 RHPZs) and it is not possible to arbitrarily reduce the sensitivity to uncertainty. A design example for this case is:

$$K_{11}(s)=\frac{-0.1}{s}, K_{22}(s)=\frac{0.7}{s}$$

The associated structural robustness is summarised in Table VI and Fig. 11.

2) Analysis with $\gamma_b(s)$: The associated MSF is

$$\gamma_b(s)=6\cdot\frac{(s+1)^2}{(s+3)(s+2)^2} \quad (25)$$

and the channels are defined as previously. The Nyquist and Bode plots of $\gamma_b(s)$ are shown in Fig. 12.

(b.1) The magnitude of $\gamma_b(s)$ while $s\rightarrow\infty$ is less than one (in fact, zero), so $1-\lim_{s\to\infty}\gamma_b(s)>0$. In this case, $\gamma_b(0)=0.5$. This implies that its Nyquist plot starts at the left side of *(1,0)*. Nevertheless, the Nyquist plot of $\gamma_b(s)$ is not always located at the left side of *(1,0)* for any frequency value.

(b.2) Function $\gamma_b(s)$ has no RHPPs and its Nyquist plot encircles *(1,0)* twice in clockwise direction; thus $(1-\gamma_b(s))$ contains *2* RHPZs.

(b.3) Notice that at low frequencies $\gamma_b(s)<1$. Then, if $K_{ij}(s)$ induce a roll–off at low frequencies $\gamma_b(s)h_j(s)$ will not encircle *(1,0)*, which in this case is desirable.

Thus, the existence of controllers reduces to the existence of $K_{ij}(s)$ which simultaneously stabilise $g_{ji}(s)(1-\gamma_b(s)h_j(s))$ and $g_{ji}(s)$ ($i,j = 1,2, i\neq j$). Nevertheless, both channels should have limited bandwidth in order to avoid the *2* encirclements to the critical point by the functions $\gamma_b(s)h_j(s)$. For instance:

$$K_{12}(s)=\frac{-6(s+2)^2(s+1)^2}{s(s+20)(s^2+0.9s+1.28)}, K_{21}(s)=\frac{-0.85\ (s+0.5882)}{s(s+1.667)}$$

The structural robustness of the channels and control system are summarised in Table VII and Fig. 13.

IV. Conclusion

The relationship between the relative gain array (RGA) and the multivariable structure function (MSF) is exposed. Under the framework of the MSF, the existence, analysis, and design of diagonal controllers for a series of plants reported in the literature are presented. In previous publications the analysis with diagonal controllers of the plants here presented was carried out by means of the RGA. So far, by using the RGA matrix only some speculation about the most convenient input–output pairing is suggested. Moreover, ill conditions of the plant –high sensitiveness to parametric uncertainty and non–minimum phase zeros– are only outlined. Here it is proved that RGA can be expressed in terms of the MSF. Furthermore, it is shown that an appropriate analysis (at low and high frequency) of the MSF gives an effective and complete framework for designing multivariable control systems. Through some examples it is shown that the MSF clarifies the possibilities to meet design specifications satisfying robustness conditions. The actual controllers and design procedures for the analysed cases are included for completeness. It is also shown that diagonal controllers exist for all possible input–output pairings, including the non–minimum phase cases. The results here presented prove that the stabilisation of the diagonal elements of **G***(s)* for stabilising diagonal controllers is not always required. Finally, robustness is described in terms of the well proven classical gain and phase margins

References

[1] E. Bristol, "On a new measure of interaction for multivariable process control, "*IEEE Trans. Automatic Control*, AC-11, pp. 133-134, 1966.

[2] G. Goodwin, S.F. Graebe, and M.E. Salgado. *Control System Design*. Prentice-Hall, USA, 2001.

[3] W.E. Leithead and J. O'Reilly, "Multivariable Control by Individual Channel Design," *Intl. Journal of Control*, 54, pp 1-46, 1991.

[4] W.E. Leithead and J. O'Reilly, "M-input M-output feedback control by Individual Channel Design," *International Journal of Control*, 56, pp 1347-1397, 1992.

[5] J. Licéaga-Castro, "Helicopter Flight Control by Individual Channel Design," Ph.D. Dissertation. University of Glasgow, UK, 1994.

[6] J. Licéaga-Castro, C. Verde, J. O´Reilly, and W.E. Leithead "Helicopter Flight Control Using Individual Channel Design," *IEEProc. Control Theory and Applications,* Vol. 142, pp 58-72, 1995.

[7] E. Licéaga-Castro and J. Licéaga-Castro, "Submarine depth control by individual channel design," *Proceedings of the 37th IEEE CDC*, 3, pp. 3183–3188, 1998.

[8] M. Morari and M. Zafiriou. *Robust Process Control*. Prentice-Hall, USA, 1989.

[9] S. Skogestad and I. Postlethwaite. *Multivariable feedback control. Analysis and design.* John Wiley & Sons, Great Britain, 1996.

[10] C.E. Ugalde-Loo, E. Licéaga-Castro, and J. Licéaga-Castro, "2x2 Individual Channel Design Matlab® Toolbox". To be presented at: *44th IEEE CDC-ECC,* Spain, 2005.

[11] E. Licéaga-Castro, C.E. Ugalde-Loo, J. Licéaga-Castro, and P. Ponce. "An efficient controller for SV-PWM VSI based on the multivariable structure function". To be presented at: *44th IEEE CDC-ECC,* Spain, 2005.

[12] C.E. Ugalde-Loo. *Control de motores de inducción utilizando la función de estructura multivariable.* MSc. Dissertation. IPN SEPI ESIME, 2005.

Table I. *Dynamical structure of closed loop channels*

Channel	Zeros	Poles
$C_1(s)$	Zeros of $(1-\gamma(s)h_2(s))$	Poles of $g_{11}(s)$, $g_{12}(s)$, $g_{21}(s)$, $h_2(s)$
$C_2(s)$	Zeros of $(1-\gamma(s)h_1(s))$	Poles of $g_{22}(s)$, $g_{12}(s)$, $g_{21}(s)$, $h_1(s)$

Table II. *Control system structural robustness assessment. Case 2 with γ_a*

Measure	$C_1(s)$	$K_{11}(s)g_{11}(s)$	$\gamma_a(s)h_2(s)$	$C_2(s)$	$K_{22}(s)g_{22}(s)$	$\gamma_a(s)h_1(s)$
BW[rad/s]	2.05	2.05	—	2.05	2.05	—
G_M [dB]	∞	∞	40	32.7	32.7	40
P_M [deg]	60.5	60.2	∞	62.9	62.6	∞

Table III. *Control system structural robustness assessment. Case 2 with γ_b*

Measure	$C_1(s)$	$K_{12}(s)g_{21}(s)$	$\gamma_b(s)h_2(s)$	$C_2(s)$	$K_{21}(s)g_{12}(s)$	$\gamma_b(s)h_1(s)$
BW[rad/s]	1.0	0.015	—	2.11	2.28	—
G_M [dB]	14	∞	-40,∞	-42,∞	∞	16.25
P_M [deg]	73	90.5	90	88	141	63

Table IV. *Control system structural robustness assessment. Case 3 with γ_a*

Measure	$C_1(s)$	$K_{11}(s)g_{11}(s)$	$\gamma_a(s)h_2(s)$	$C_2(s)$	$K_{22}(s)g_{22}(s)$	$\gamma_a(s)h_1(s)$
BW[rad/s]	2.07	1.89	—	2.04	1.84	—
G_M [dB]	∞	∞	∞	52.9	53.6	∞
P_M [deg]	60.3	72.2	∞	64.8	77.2	∞

Table V. *Control system structural robustness assessment. Case 3 with γ_b*

Measure	$C_1(s)$	$K_{11}(s)g_{11}(s)$	$\gamma_a(s)h_2(s)$	$C_2(s)$	$K_{22}(s)g_{22}(s)$	$\gamma_a(s)h_1(s)$
BW[rad/s]	2.09	0.568	—	1.93	0.834	—
G_M [dB]	∞	∞	∞	∞	∞	10.17
P_M [deg]	72.5	107	96	69.4	87.4	59

Table VI. *Control system structural robustness assessment. Case 4 with γ_a*

Measure	$C_1(s)$	$K_{11}(s)g_{11}(s)$	$\gamma_a(s)h_2(s)$	$C_2(s)$	$K_{22}(s)g_{22}(s)$	$\gamma_a(s)h_1(s)$
BW[rad/s]	0.103	0.1	—	0.521	0.65	—
G_M [dB]	8.17	∞	∞	17.2	17	21.82
P_M [deg]	56.9	98	124	57.5	60	41

Table VII. *Control system structural robustness assessment. Case 4 with γ_b*

Measure	$C_1(s)$	$K_{12}(s)g_{21}(s)$	$\gamma_b(s)h_2(s)$	$C_2(s)$	$K_{21}(s)g_{12}(s)$	$\gamma_b(s)h_1(s)$
BW[rad/s]	*1.28*	*1.33*	—	*0.322*	*0.705*	—
G_M [dB]	*∞*	*∞*	*6.02*	*∞*	*∞*	*6.02*
P_M [deg]	*74.7*	*41.1*	*∞*	*95.8*	*82*	*34*

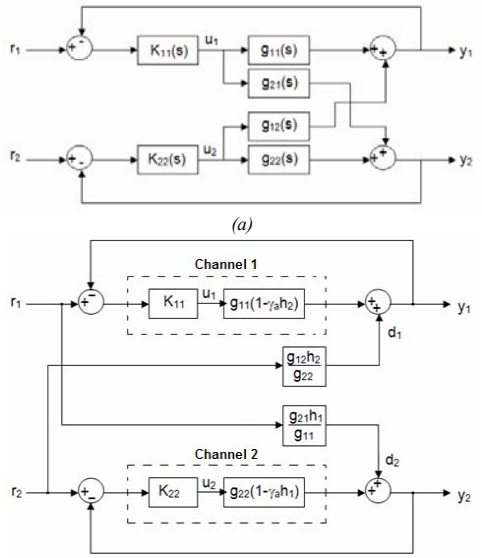

Fig. 1. *(a) 2-input 2-output system with a diagonal controller. (b) Equivalent channel representation*

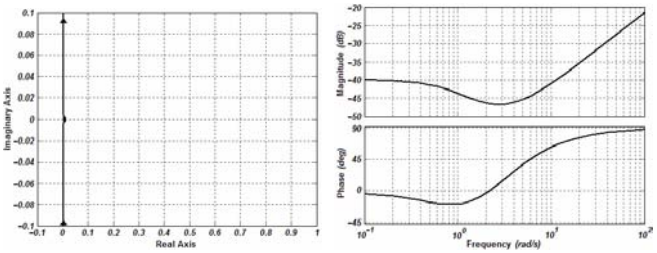

Fig.2. *Assessing $\gamma_a(s)$ structure. Case 2:(a) Nyquist and (b) Bode diagrams*

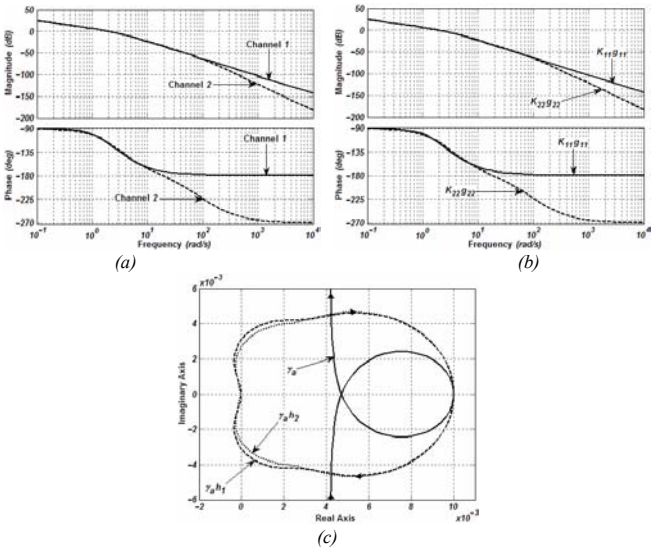

Fig.3. *Control system structural robustness assessment. Case 2 with $\gamma_a(s)$. Bode diagrams:(a)C_1,C_2;(b)$K_{11}g_{11},K_{22}g_{22}$; Nyquist diagram:(c)$\gamma_a h_2$, $\gamma_a h_1$*

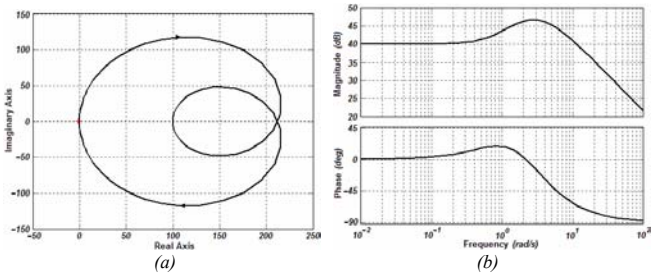

Fig. 4. *Assessing $\gamma_b(s)$ structure. Case 2:(a) Nyquist and (b)Bode diagrams*

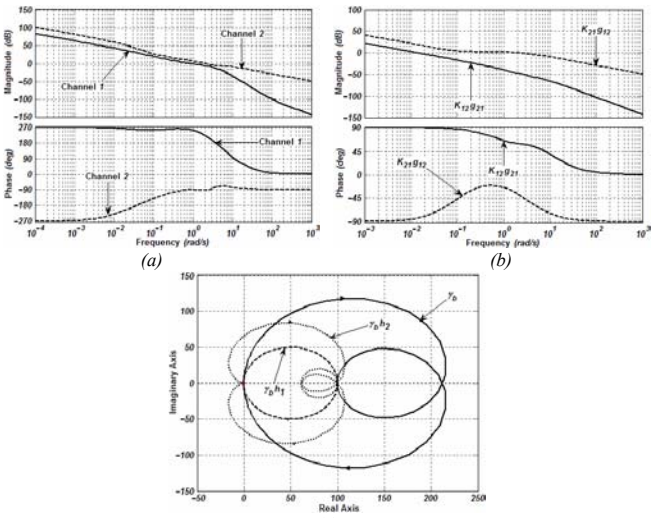

Fig.5. *Control system structural robustness assessment. Case 2 with $\gamma_b(s)$. Bode diagrams:(a)C_1,C_2;(b)$K_{12}g_{21},K_{21}g_{12}$; Nyquist diagram:(c)$\gamma_b h_1,\gamma_b h_2$*

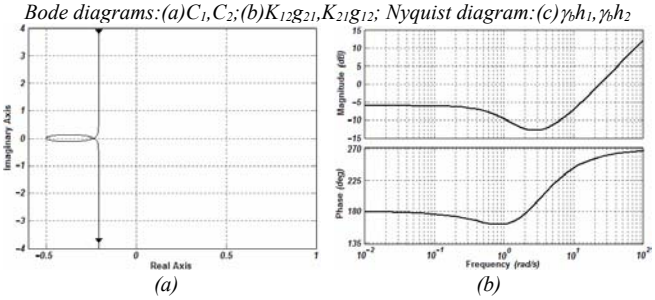

Fig. 6. *Assessing $\gamma_a(s)$ structure. Case 3: (a) Nyquist and (b) Bode diagram*

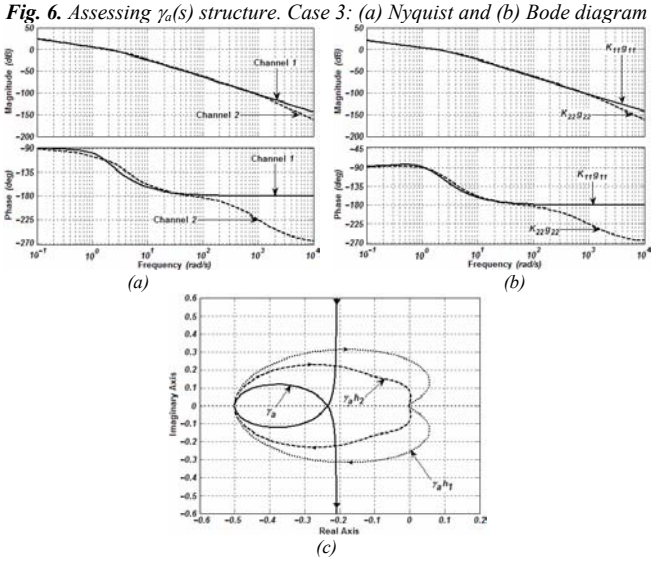

Fig.7. *Control system structural robustness assessment. Case 3 with $\gamma_a(s)$. Bode diagrams:(a)C_1,C_2;(b)$K_{11}g_{11},K_{22}g_{22}$; Nyquist diagram:(c)$\gamma_a h_2$, $\gamma_a h_1$*

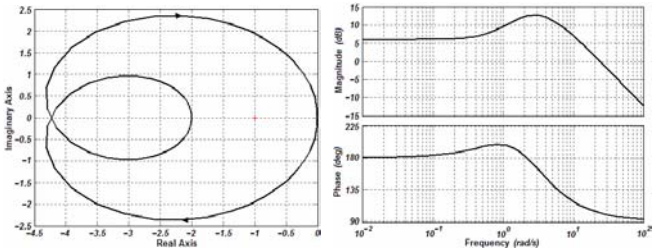

(a) (b)

Fig. 8. *Assessing $\gamma_b(s)$ structure. Case 3: (a) Nyquist and (b) Bode diagram*

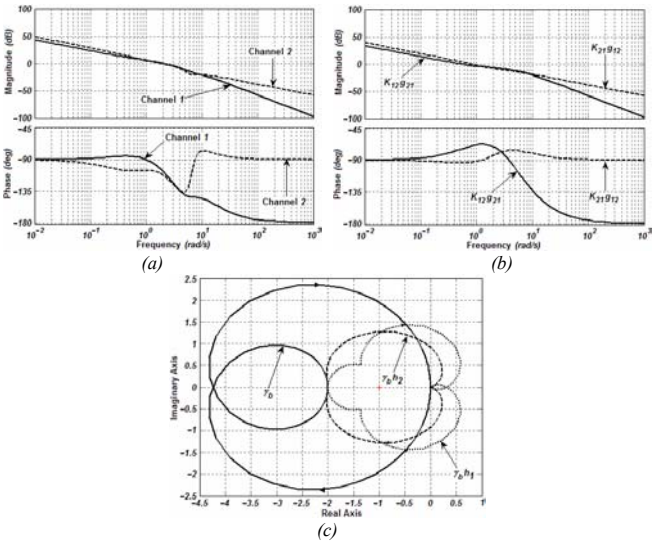

(a) (b) (c)

Fig.9. *Control system structural robustness assessment. Case 3 with $\gamma_b(s)$. Bode diagrams:(a)C_1,C_2;(b)$K_{12}g_{21},K_{21}g_{12}$; Nyquist diagram:(c)$\gamma_b h_1$, $\gamma_b h_2$*

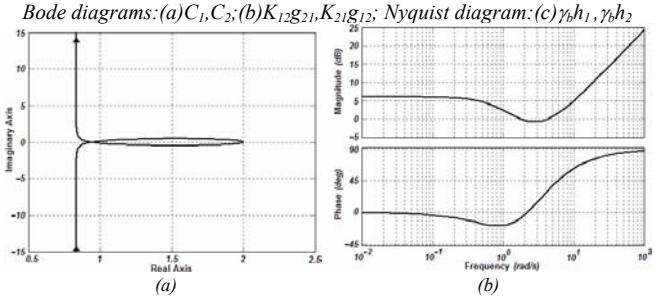

(a) (b)

Fig.10. *Assessing $\gamma_a(s)$ structure. Case 4: (a)Nyquist and (b)Bode diagram*

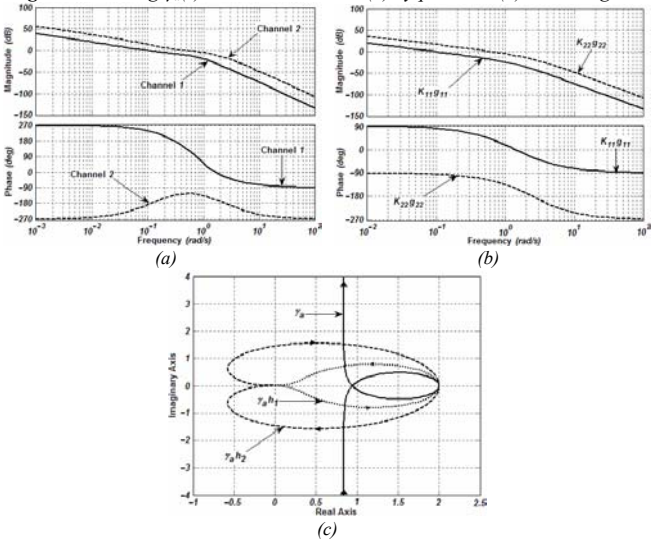

(a) (b) (c)

Fig.11. *Control system structural robustness assessment. Case 4 with $\gamma_a(s)$. Bode diagrams:(a)C_1,C_2;(b)$K_{11}g_{11},K_{22}g_{22}$; Nyquist diagram:(c)$\gamma_a h_2$, $\gamma_a h_1$*

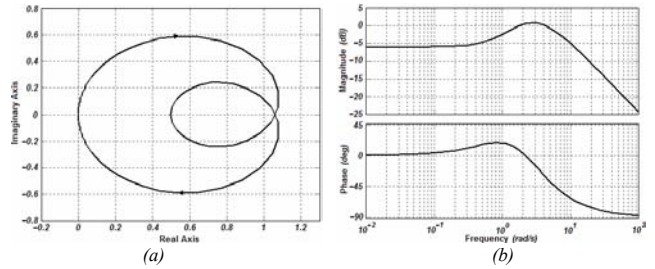

(a) (b)

Fig.12. *Assessing $\gamma_b(s)$ structure. Case 4: (a)Nyquist and (b)Bode diagram*

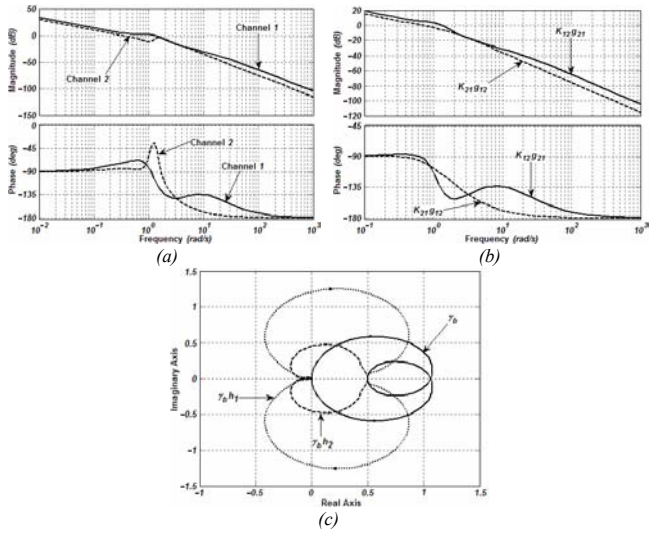

(a) (b) (c)

Fig.13. *Control system structural robustness assessment. Case 4 with $\gamma_b(s)$. Bode diagrams:(a)C_1,C_2;(b)$K_{12}g_{21},K_{21}g_{12}$; Nyquist diagram:(c)$\gamma_b h_1$, $\gamma_b h_2$*